CHAPTER 2

Superficial Fabrication of Gold Nanoparticles Modified CuO Nanowires Electrode for Non-enzymatic Glucose Detection

Contents

*Part of this work has been published as:

1. Mishra, Ashwini Kumar, et al. "Superficial fabrication of gold nanoparticles modified CuO nanowires electrode for non-enzymatic glucose detection." *RSC advances* 9.4 (2019): 1772-1781.
2. Mishra, Ashwini Kumar, et al. "Au nanoparticles modified CuO nanowire electrode based non-enzymatic glucose detection with improved linearity." *Scientific reports* 10.1 (2020): 1-10.

CHAPTER 2

Superficial Fabrication of Gold Nanoparticles Modified CuO Nanowires Electrode for Non-enzymatic Glucose Detection

2.1 Introduction

It has been discussed in chapter1 that the enzyme-based sensors are more costly, its stability is poor, and it is also affected by working temperature, relative humidity and the pH value [72]. Due to the reasons mentioned above, Non-enzymatic based glucose sensors will be studied in this chapter. The sensing mechanism of the non-enzymatic-based glucose sensors is totally different from enzymatic-based glucose sensing. In non-enzymatic based glucose sensing, electrocatalysts are required, which satisfy some necessary conditions like outstanding conductivity, large surface area, and high electro-catalytic property, effective electron transfer between electrocatalysts to the conductive substrate, good selectivity, high stability, and good reproducibility[41]. As discussed in the chapter1, researchers have investigated various metal oxides like Co3O4, NiO, ZnO, Cu2O, MnO2, Fe2O3 Ag2O, and SnO2 for glucose sensing applications due to low fabrication cost [72]. Among the various metal oxides based glucose sensors, CuO (copper oxide) is considered to be suitable sensing for glucose sensors applications because of its low fabrication cost, facile fabrication, abundant availability in nature, and good catalytic properties [39], [41], [57], [92], [62], and [68].

CuO is a p-type semiconductor with a bandgap of 1.2eV. CuO is used in many applications such as gas sensors, electrochemical sensors, photoelectric devices, and

lithium-ion batteries due to its exciting properties [93]-[96], [102].

The CuO nanostructures grown on conducting copper foil by simple and facile route can be used as low-cost glucose sensors with high sensitivity, fast response, and stable detection due to its better catalytic property over other metal oxide nanostructures [72].

As discussed in Chapter1 that only metals (Pt, Au, Ni, etc.) based electrodes have been reported for glucose sensing applications. The main disadvantage of these noble metal-based glucose sensors is their cost. Nobel metal can be used as a co-catalyst for glucose sensing with a metal oxide-based (catalyst) glucose sensor. A metal oxide is preferred due to its catalytic property, and noble metal is preferred for its high conductive properties [97].

In this chapter, we will study the enhanced catalytic properties, and fast direct electron transfer through the CuO NWs in the presence of Au NPs have been explored for the drastic improvement in the sensitivity and linear range of the glucose sensor. In this study, NaOH has been taken as a solute. For good sensitivity, a NaOH concentration of 0.1 M has been used, while for better linearity, 0.5 M and 1 M NaOH concentrations have been taken for the observation. This is the following reason why the sensitivity and linearity are controlled by NaOH concentration.

Incipient hydrous oxide adatom mediator (IOHAM) model has been explored for the complex electrocatalytic behavior of the glucose [101]. IOHAM model explains the consequences of the active hydroxide anions in the domain of electrode surface formed by the separation of water to the electro-oxidation of glucose and additional organic compounds.

$$H_2O \rightarrow H^+ + OH^- \qquad (2.1)$$

Further, according to the following equation, the chemisorption of hydroxide anions to the reductive metal adsorption site (M) leads to the generation of oxidative adsorbed hydroxide radical (MOHads) [101]:

$$M^+ + OH^- \rightarrow MOH_{ads} \qquad (2.2)$$

From Equations (2.1) and (2.2), it is concluded that MOHads creations are increased by increasing in the concentration of OH-. Therefore, non-enzymatic glucose detection is a pH-dependent process, and highly alkaline surroundings improve its sensitivity [101]. Due to the reason mentioned above, at a higher concentration of NaOH, the sensitivity and linearity are improved drastically. Concentration of the solute (NaOH) determines the sensitivity and linearity of the glucose sensors. Following reaction takes place during the experiment [39]:

$$CuO + H_2O + 2OH^- \rightarrow Cu(OH)_4^- + e^- \qquad (2.3)$$

$$Or \quad Cu(II) + OH^- \rightarrow Cu(III) + e^-$$

$$Glucose \rightarrow Gluconolactone + e^- \qquad (2.4)$$

$$Cu(III) + e^- \rightarrow Cu(II) \qquad (2.5)$$

Cu(III) + Glucose→ Gluconolactone +Cu(II) and Gluconolactone →Glucononic Acid (Hydrolysis) (2.6)

In equation (2.3), Copper (II) has been oxidized into Copper (III) in alkaline medium. More concentration of the solvent causes more oxidation of the copper surface which can again be reduced into copper (II) in the presences of glucose.

Moreover the projected sensor is also used for detection of glucose in human blood and its result has been compared with commercial available glucose sensors. Closed matching of this sensor with commercial available sensor shows that our sensor can be used for the practical application.

2.2. Experimental Details

2.2.1. Electrodes Preparation

2.2.1.1. Preparation of $Cu(OH)_2$ NWs Electrode

Small squares (5 mm × 5 mm) of copper foil were used as the starting material for electrodes. These copper foils are cleaned ultrasonically in DI water, HCl, acetone, and isopropanol sequentially. Then foils were immersed in a solution consisting of 80 µl of 10 M NaOH, 180 µl of H_2O, and 40 µl of 1 M $(NH_4)_2S_2O_8$. After 30 minutes, the foils were taken out from the solution and kept for drying in the presence of air. A deep blue film formed of Cu $(OH)_2$ NWs on Cu foil [39]. Electrode preparation process of Cu $(OH)_2$ NWs is shown in figure1. (a).

$$Cu(s) + 4NaOH(aq) + (NH_4)_2S_2O_8(aq) \rightarrow Cu(OH)_2(s) + 2Na_2SO_4(aq) + 2NH_3(g) + 2H_2O \quad (2.7)$$

The overall mechanism for the formation of $Cu(OH)_2$ NWs can be described as follows. During the synthesis, the copper layer on the top of the copper foil serves two purposes: supplies copper required for $Cu(OH)_2$ growth and provides nucleation sites for the formation of 1D structures on the surface. The presence of ammonium persulfate enhances the $Cu(OH)_2$ growth mechanism by allowing for fast oxidation of the copper surface [102]. Though the sodium hydroxide can also oxidize copper surfaces, however, it takes longer time [102]. $Cu(OH)_2$ is thus formed on the substrate when the liberated Cu^{2+} cations react with the hydroxide anions (OH_) present in the solution. Gas bubbles arise throughout the reaction, and a distinct ammonia odour can be detected, suggesting the creation of NH_3. The overall chemical equation is summarized in equation (2.7)[102].

The growth rate of $Cu(OH)_2$ is inversely proportional to the inter-planar distance, according to the Bravais–Friedel–Donnay–Harker law. Since the inter-planar distance of (100) is the smallest, the copper hydroxide grows significantly quicker along (100) than in the other directions to result in the creation of 1D structures of Cu $(OH)_2$ nano wires [102]. After the heat treatment, the Cu $(OH)_2$ NWs are converted into CuO NWs.

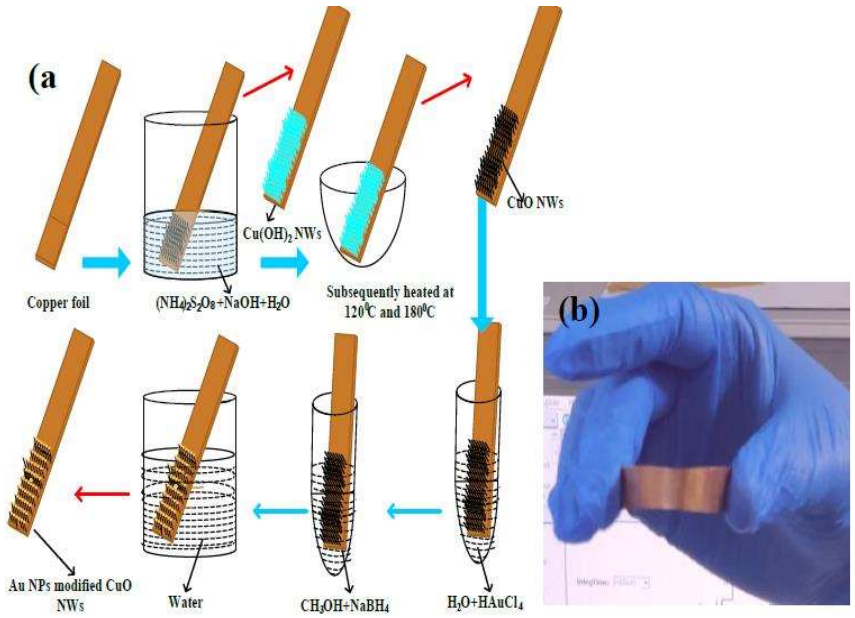

Figure 2.1: (a) Fabrication step of gold modified CuO NWs on Cu foil electrode, and (b) bendable copper foil

2.2.1.2. Preparation of CuO NWs Electrode

The obtained $Cu(OH)_2$ NWs grown on Cu foils were kept on an alumina boat and put inside the furnace with the flow of argon gas (Ar) for 30 minutes. After 30 minutes, the flow of argon gas was stopped, and in the presence of Ar atmosphere, the foils were heated to 120°C for three hours. Further, the foils were heated to 180°C for 2 hours to promote crystallization. The blue film got converted into the black film of CuO nanowire [39].

$$Cu(OH)_2 \rightarrow CuO + H_2O \tag{2.8}$$

2.2.1.3. Preparation of gold nano particle modified CuO NWs electrode

The obtained black-colored CuO NWs were the first dipped in a solution containing 8 mg chloroauric acid (HAuCl4) in 3 ml DI water for 10 minutes. Afterward, these foils

were immersed in a solution consisting of 9 mg sodium borohydride (NaBH4) dissolved in a 3ml methanol solvent. Finally, the foils were rinsed with DI water for 2 minutes to obtain gold NPs (GNPs) modified CuO NWs electrodes. The reactions for the formation of gold nanoparticles are obtained with modification as [103]-[104].

$$NaBH_4 + 4CH_3OH \Leftrightarrow NaB(OCH_3)_4 + 4H_2 \tag{2.9}$$

$$4HAuCl_4 + 3NaBH_4 \rightarrow 4Au + 6H_2 + 3NaCl + 3BCl_3 + 4HCl \tag{2.10}$$

2.2.2. Electrode Characterizations and Electrochemical Set-up

The crystal structure and phase of the electrode materials were identified using X-ray diffraction (XRD) (RIGAKU-Smart XDMAX, PC-20, 18-kW Cu rotating anode, Rigaku, Tokyo). The surface morphology of copper foil, Cu(OH)2 NWs, CuO NWs, and Au NPs modified CuO NWs were investigated by scanning electron microscopy (SEM) ((Model: EVO MA 15/18 from Carl Zeiss Microscopy Ltd., UK). The Au NPs modified CuO NWs were examined by high-resolution transmission electron microscopy (HRTEM) and scanning transmission electron microscopy (STEM) (FEI G2 T20 STWIN). Electrochemical measurements were performed in a 3-electrode electrochemical cell configuration (BAS100B electrochemical workstation) with four different CuO-based electrodes as working electrodes, a platinum wire as a counter electrode, and Ag/AgCl as a reference electrode, as shown in Fig. 2.2. A solution of 0.1 M NaOH in DI water is used as an electrolyte for the cyclic voltammetry measurement at room temperature.

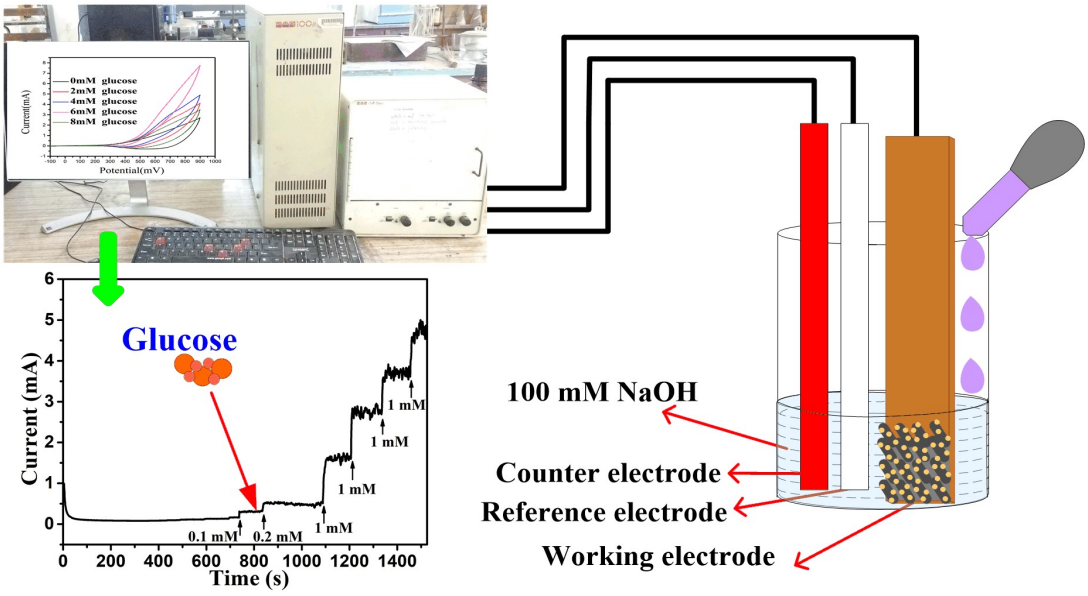

Fig.2.2. Electrochemical set-up for the detection of glucose

2.3. Results and Discussions

2.3.1. Characterizations of Electrodes

2.3.1.1. XRD characterization of the Electrode

The XRD patterns of Cu foil, Cu(OH)2 NWs, CuO NWs, and Au NPs modified CuO NWs have been compared with standard JCPDS file numbers 04-0836, 35-0505, 80-1917, and 04-0784 of Cu, Cu(OH)2, CuO, and Au, respectively as shown in Fig. 3. The sharp crystalline peaks found at 43.37 degree, 50.61 degree, and 74.27 degree correspond to (111), (200), and (220) of FCC Cu, confirming the composition of the foil as shown in figure 3(a). The other two minor peaks at 35.39 degrees and 38.65 degrees are due to impurities of the native oxide of copper. The XRD of Cu(OH)2 NWs sample shown in Fig. 3 (b) matches well with the orthorhombic phase (JCPDS card # 35-0505), thereby confirming the successful growth of Cu(OH)2 NWs on the Cu foil. Heating-

induced de-hydroxylation leads to recrystallization and formation of CuO nanowire, as evident from the XRD plot (JCPDS card # 80-1917) shown in Fig. 3(c). The comparison of the XRD pattern of the Au NPs modified CuO NWs in Fig. 3 (d) with those of CuO and Au confirms that other minor peaks in the XRD of the Au NPs decorated CuO NWs result from the small amount of Au NPs grown on the CuO NWs.

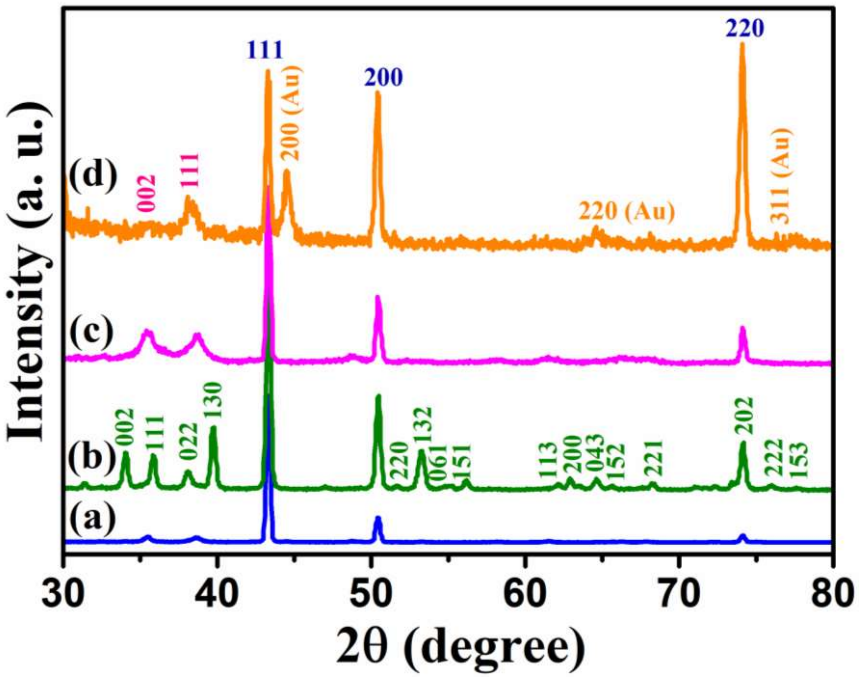

Figure.2.3. The XRD pattern of (a) Cu electrode, (b) Cu $(OH)_2$ NWs electrode, (c) CuO NWs electrode, and (d) Au NPs modified CuO NWs electrode

2.3.1.2. SEM Image Characterizations of Electrodes

The surface morphology obtained for various electrodes such as Cu, Cu(OH)2 NWs grown on Cu foil, CuO NWs has grown on Cu, and Au NPs modified CuO NWs grown on Cu are shown in Fig. 2.4 (a)-(d). The SEM images of the copper foil in Fig. 2.4 (a) show that the copper foil is loutish. The wire-like morphology of Cu (OH) 2 with an average diameter of 150-350 nm uniformly covering over the copper foil is observed in

the SEM image shown in Fig.2.4 (b). The SEM image in Fig. 2.4 (c) shows uniformly distributed CuO NWs (of the average diameter of 100-300 nm) on Cu foil. This wide variation in the diameter of CuO NWs may be due to in-situ attached two NWs, which cannot be distinguished by SEM because of its low-resolution limitation. Finally, the surface morphology of Au NPs modified CuO NWs under study is shown in Fig.2.4 (d). The SEM image in the figure shows the non-uniform distribution of Au NPs on the CuO NWs.

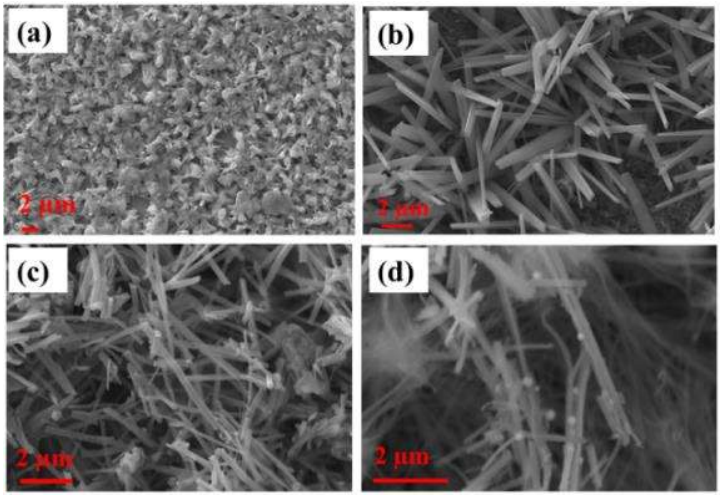

Figure 2.4. The SEM images of (a) Cu electrode, (b) $Cu(OH)_2$ NWs electrode, (c) CuO NWs electrode, and (d) Au NPs modified CuO NWs electrode.

2.3.1.3. TEM Characterizations of Electrodes

The surface morphology of the Au NPs modified CuO NWs understudy is further investigated by HRTEM analysis as shown in Figure. 2.5. The bright-field image of Au NPs over freestanding CuO NWs is shown in Figure 2.5(a). The image clearly shows the well-distributed Au NPs on CuO NWs substrate as small dark dots. The mass-thickness contrast (higher atomic weight of Au as compared to the average atomic weight of Cu and O) is the reason for the dark appearance of the Au nanoparticles. The average diameter of the CuO NWs and Au NPs are 75-125 nm and 10-15 nm,

respectively. The lengths of the CuO NWs are 1-2 μm. The selected area electron diffraction (SAED) pattern of the Au NPs modified CuO NWs taken from the scanning image area is shown in Figure. 2.5(b). The diameter of the first three concentric circles corresponds to CuO (002), CuO (111)/Au (111), and CuO (202) with d-spacing of 2.5 Å, 2.32 Å, and 1.58 Å, respectively. The amount of Au is very less, so it is not possible to confirm the presence of Au using the SAED pattern. The single nanowire is considered from the High-resolution transmission electron microscopic (HRTEM) of Figure. 2.5 (a) and shown in Figure.2.5 (c). It is observed that the Au NPs are well distributed over CuO NWs, as shown in Figure. 2.5(c). The highly dense Au NPs on the CuO NWs are observed in our earliest result, shown in Figure.2. 6. The further magnified image is shown in Figure.2. 5 (d), where the brighter, smoother parts are of CuO NWs, and dark dots are of Au NPs. The inset image of Figure. 2.5 (d) shows the lattice spacing measurements for white and dark regions as 2.5 Å and 2.32 Å, respectively, which confirm the presence of CuO (002) and Au (111). The d-spacing calculation using HRTEM is shown in Figure. 2.7 and Figure.2.8.

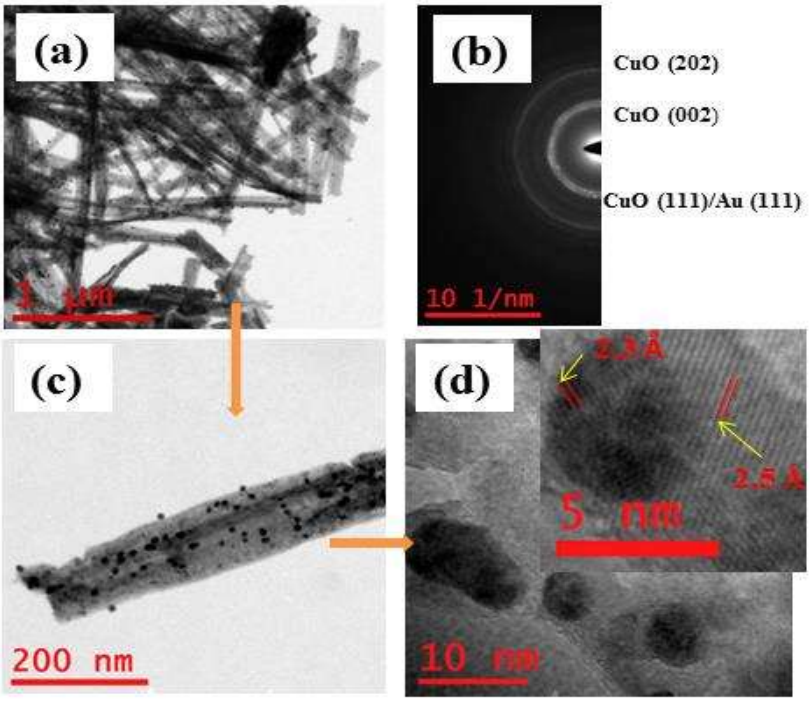

Figure. 2.5. (a) The TEM images of free-standing Au modified CuO NWs; (b) SAED pattern of selected area, (c) TEM image of single Au NPs modified CuO NWs, (d) HRTEM image for Au NPs and CuO NWs (Further magnified version is view in inset for d-spacing evaluation).

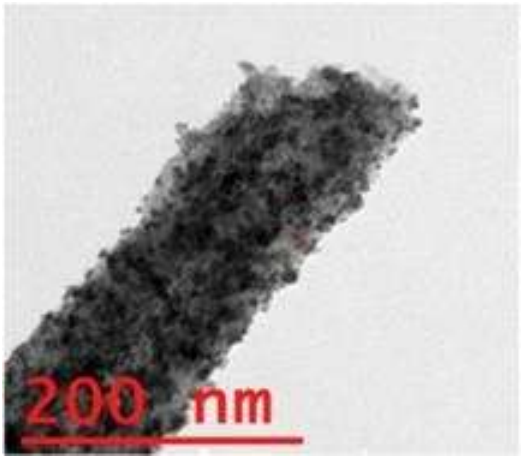

Figure.2.6. TEM image of Au NPs modified CuO NWs

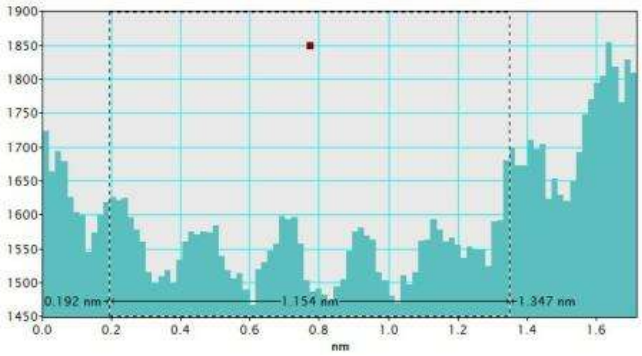

Figure.2.7. Calculation of d-spacing for CuO NWs

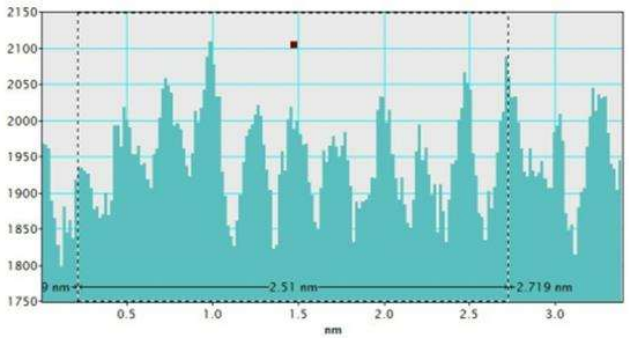

Figure. 2.8. Calculation of d-spacing for Au NPs.

The STEM analysis of Au NPs modified CuO NWs is shown in Figure.2. 9. Figure. 2.9 (a) is the image of single CuO NWs along with Au NPs using STEM-HAADF (high angle annular dark field). Small white dots are due to the high atomic weight of Au NPs, which is easily obtained from Z-contrast using HAADF. Figure.2.9 (b) is the magnified view of Figure. 2.9(a), where the distributions of Au NPs over CuO NWs are clearly seen. The yellow dotted region in Figure.2. 9 (c) confirms the presence of CuO NWs, whereas the violets doted region in Figure.2. 9 (d) confirm the presence of Au NPs. The EDS mapping is shown in Figure2.9 (e) confirms the presence of elements such as Cu, O, and Au in the composite. It is easily observed from the EDS mapping that the amount of Au NPs as compared to CuO NWs is significantly less.

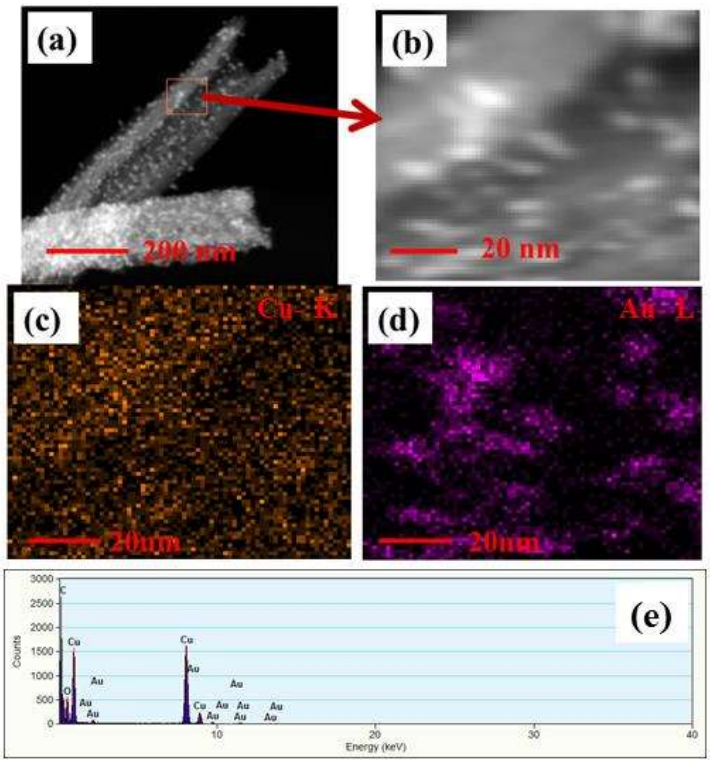

Figure.2.9 (a) The HAADF-STEM images of single free-standing Au modified CuO NWs, (b) Magnified view of STEM image with zoomed Au NPs and CuO NWs, (c) Mapping of CuO NWs, (d) Mapping of Au NPs, and (e) EDS spectrum of the selected area

2.3.1.4. XPS Characterizations of the Electrodes

The characterization details of the surface composition of CuO NWs and CuONWs with GNP (gold nanoparticles) are shown in Figure. 2.10. The whole spectrum of CuO NWs GNP shows the presence of Cu, O, Au, C, and Na atoms, which are shown in Figure. 2.10(a). The high resolutions spectra for O 1s are shown in Figure. 2.10(b), which depicts two peaks in CuO NWs GNP at 531.16 eV and 532.27 eV equivalent to the oxygen vacancies or defect (OV)present because of O2 species in the lattice (OL) and dissociated (OC) oxygen species [105]-[107]. The XPS of Cu 2p core level two peaks of energy 934 eV and 954eV are shown in Figure.2.10(c), which corresponds to Cu 2p3/2 and Cu 2p1/2 respectively, which confirms the existence of the Cu+2. Two more peaks

present at 941.8 eV and 961.9 eV are the satellite peaks of Cu2p3/2 and Cu2p1/2, respectively shows the presence of an unfilled shell of 3d9, and it again proves the presence of Cu+2 in the sample. Gold (Au) 4f core of the Au/CuO nanostructure (shown in figure 2.10 (d) has been filled with two peaks, i.e., Au 4f7/2 and Au 4f5/2 with binding energy 84.0eV and 87.7eV, which prove the presence of gold on CuO nanowires.

For the selection of the better electrode the different copper oxide were chosen like Cu $(OH)_2$NWs, CuO NWs and CuO NWs with GNP. The current which is observed in the case of $Cu(OH)_2$ NWs is very low, moderate for CuO NWs and extremely high for CuO NWs with GNP in the solution of 0.5M NaOH and 1mM glucose concentrations.

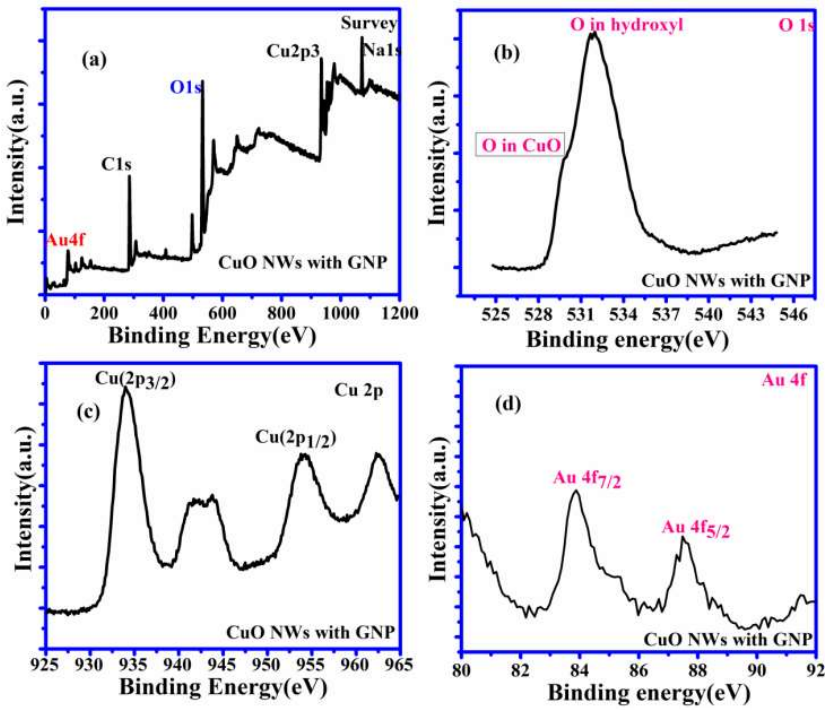

Figure 2.10. XPS analysis. (a) XPS spectrum of CuO NWs with GNP showing full scan survey (b) and corresponding de-convoluted peaks in the high-resolution spectra for O 1s (c) Cu 2p (d)Au 4f.

2.3.2. Electro-Catalytic Ability of Electrodes towards Glucose Oxidation

The working electrode CuO NWs get oxidized electrochemically to form Cu(III) species such as $Cu(OH)_4^-$ or CuOOH [39]:

$$CuO + H_2O + 2OH^- \rightarrow Cu(OH)_4^- + e^-$$

Or,

$$Cu(II) + OH^- \rightarrow Cu(III) + e^- \quad (2.3)$$

It is reported that oxidation of glucose is enhanced in the presence of copper and its compounds due to strong catalytic behaviour [68]. Following chemical reaction take place for the oxidation of glucose under Cu (III) [23], [98], [109]:

$$Glucose \rightarrow Gluconolactone + e^- \quad (2.4)$$

$$Cu(III) + Glucose \rightarrow Gluconolactone + Cu(II) \quad (2.5)$$

And, Gluconolactone →Glucononic Acid (Hydrolysis)

(2.6)

The above reaction mechanism is also shown in figure 2.11. (a). Similarly, the Au NPs modified CuO NWs electrode also participates in the reaction mechanism, as shown in figure 2.11 (b). Thus, the overall oxidation of glucose has been increased. It may also be noted that the glucose oxidation reaction is not spontaneous, and it is catalyzed by Cu(III) and/or Au(I). These two species formed in-situ through electrochemical hydrolysis process as Cu(II) →Cu(III) +e- (Redox potential -2.41 V) and Au(0) → Au(I) +e- (Redox potential -1.83 V). This step is followed by glucose oxidation, which is oxidized to gluconolactone (Redox potential -0.32 V). The above

formation of gluconolactone is feasible by the Cu(III) and/or Au(I). Even though this gluconolactone is more feasible for Cu(III) mediated reaction as apparent from the redox potential value, but the rate-determining step of the overall reaction is the formation of Cu(III) or Au(I). Since the formation of Au (I) is more feasible than Cu (III), Au gives a higher oxidation rate of glucose. Au and CuO interface plays a significant role in this overall electrochemical oxidation process as it impacts the charge transport from the Au NPs to Cu foil through CuO NWs. The negligible energy barrier between Au/CuO is seen in Figure. 2.11 (c) ensures that impediment in the electron transfer is minimum. Apart from these catalytic comparisons of the CuO and Au, the hybrid structure of the electrode is also very much favorable for the oxidation of glucose because of the enhanced surface area due to the 3D electrode structure, low-cost electrode using the loading of very less amount of Au NPs, and the large increase in reactive centers due to larger surface to volume ratio of the Au NPs. The complete process of glucose oxidation and charge transfer is described in figure.2. 11. When the glucose is introduced in 0.1 M NaOH solution, it gets oxidized in the catalytic presence of CuO/Au, and this electrochemical reaction releases an electron. The released electron moves to the conduction band (CB) of CuO NWs through Au NPs. Further, this electron moves in the Au-CuO-Cu electrode network as Solid-state charge transfer, as shown in Figure.2.11 (c)

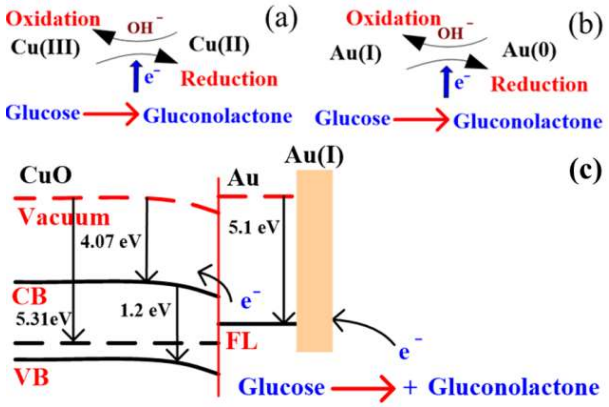

Figure.2.11. (a) Glucose detection mechanism in CuO, (b) Glucose detection mechanism in Au, and (c) Glucose detection mechanism in CuO NWs/AuNPs structure under applied potential.

2.3.3. Determination of Electrolyte Concentration (NaOH)

It is found that CuO NWs have the highest electrocatalytic performance when 0.1 M NaOH solutions are used as electrolytes, similar to ref.[39]. We have also observed that similar to CuO NWs electrode, Au NPs modified CuO NWs have the highest electrocatalytic properties when 0.2 M NaOH is used as an electrolyte, as shown in Figure.2.12. But more basic solution results at 0.2M NaOH as a comparison of the 0.1 M NaOH. For obtaining a large amount of current with less concentration of the solvent results, 0.1M NaOH was chosen as a solvent. An optimized scan rate of 50 mV/s was taken in the entire work, otherwise stated. In view of the above, the electrocatalytic behaviors of various electrodes have been investigated in the 0.1 M NaOH electrolyte solution in the potential range from -0.1 to 0.9V.

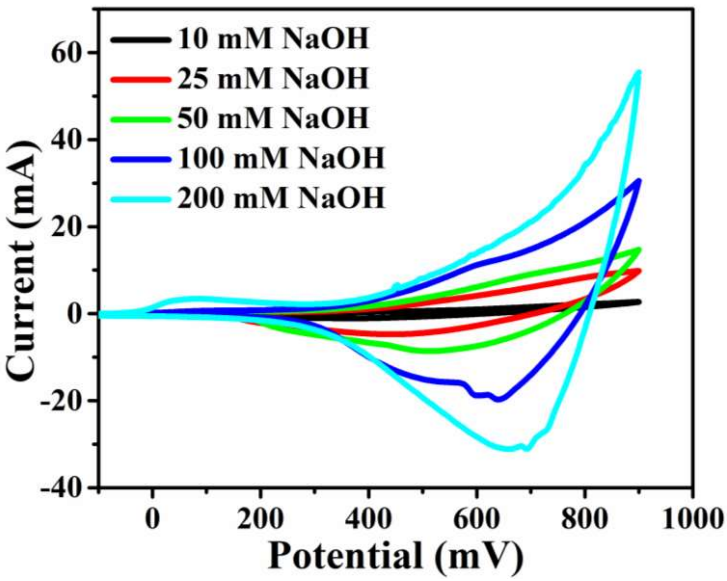

Figure.2.12. Electrocatalytic effect of different concentration of NaOH (a) 10 mM, (b) 25 mM, (c) 50 mM, (d) 100 mM, and (e) 200 mM with scan rate100 mV/s.

2.3.4. Determination of Suitable Electrode for Glucose Sensing

A fixed amount of 4 mM of glucose is used for all electrodes. It is found that the oxidation current increases with the amount of glucose in the electrolyte for all the electrodes, as shown in Figure. 2.13. The amount of change in oxidation current due to glucose in $Cu(OH)_2$ NWs is 1.11 times higher than the bare Cu electrode. This increase in oxidation current is due to the effective surface-to-volume ratio for $Cu(OH)_2$. On the other hand, the change in oxidation current in the case of the CuO electrode is 1.77 times higher than Cu $(OH)_2$ electrode. Further 2.86 time's enhancement in the change in oxidation current is observed when Au NPs modified CuO NWs electrode was used as the working electrode. This enhancement in oxidation current is attributed to the gradual increase in the surface to volume ratio in Cu (OH)2 NWs, CuO NWs, and Au NPs modified CuO NWs. We also investigated the current response of the Au NPs modified

CuO NWs electrode at different concentrations of glucose varying from 0 mM to 8 mM by adding in the electrolyte.

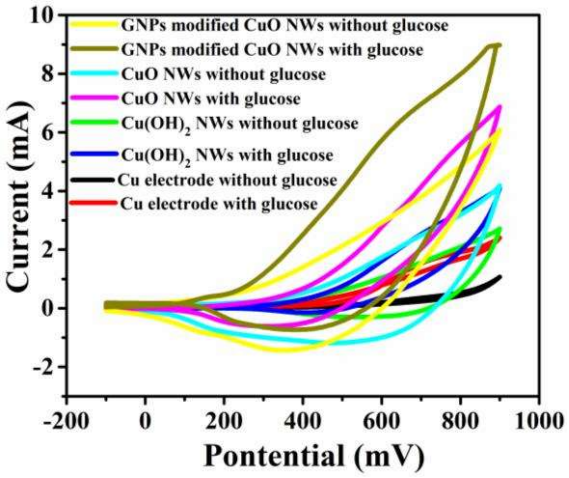

Figure. 2.13. C-V plots of Cu, Cu $(OH)_2$ NWs, CuO NWs, and Au NPs modified CuO NWs electrodes at 0 mM and 4mM of glucose, respectively

We have observed a proportional increment in the current with the increase in the glucose, as shown in Fig. 2.13. The transient current response is also investigated for a potential window from 0.4 V to 0.7 V obtained by successive adding 0.25 mM of glucose in the 0.1 M NaOH electrolyte. The variation of current with glucose concentration is shown in figure 2.13.

Table.2.1. Comparison of CuO Nano-Materials-Based Glucose Sensors.

Type of Electrodes	Detection Limit (µM)	Sensitivity ($\mu AmM^{-1}cm^{-2}$)	Linear range(mM)	References
CuO NWs	0.05	1886.3	0.002-3.56	[72]
CuO NWs/Cu foam	0.3	2217.4	0.001-18.8	[41]
CuO nanosphere	1	404.53	0-2.55	[62]

CuO flowers	4	709.52	0.004-8	[71]
Ag NPs/CuO nanofibers	0.052	1347	0.0005-0.5	[93]
CuO nanofibers	0.8	431.3	0.006-2.5	[25]
CuO nanoplatelets	0.5	3490.7	Up to 0.8	[108]
CuO nanourchins	1.97	1634	Up to 5	[111]
Sandwich-structured CuO	1	5342.8	0-3.2	[112]
CuO nanothorn arrays	0.275	5984.3	0.0002-2	[113]
CuO nanostructure	49	1620	Up to 4	[114]
CuO/TiO_2 nanotube	1	79.9	0-2	[115]
CuO-ZnO nanorods	0.4	2961.7	Up to 8.45	[116]
Au/CuO nanocauliflowers	0.3	708.7	0.001-30	[97]
Au/CuO nanohybrids	2.8	374	Up to 12	[117]
Au NPs modified CuO NWs	**0.5**	**4398.8**	**0.0005-5.9**	**This work**

2.3.5. Transient Current Response towards Glucose at Working Potential of 0.6 V

Based on the results shown in Figure.2.14, the Au NPs modified CuO NWs electrodes are used as working electrodes for electrochemical measurement at an applied bias of 0.6V. To ensure enough sensitivity and a lower background current, the effect of applied potential was also investigated by three successive amperometric measurements of 0.25 mM glucose into a stirring 0.1 M NaOH at different potentials ranging from 0.4 V to 0.7 V. As shown in Fig.2.14 of the thesis, the most significant response sensitivity is obtained at 0.6 V. As a result, 0.6 V was applied as the working potential for the subsequent amperometric measurements.

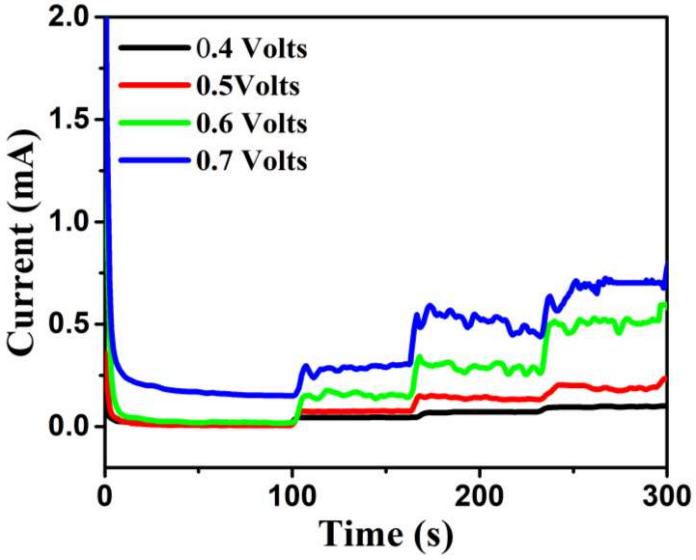

Figure.2.14. Transient current responses of Au NPs modified CuO NWs at different working potentials and successive additions of 0.25 mM glucose into 0.1 M NaOH solution.

2.3.6. Electrode Performance towards the Different Glucose Concentration

The detection limit and sensitivity were found as 0.5 µM and 4398.8 µAmM-1cm-2, respectively, which are better than the results reported by others [97], [101], [111]. The various sensor parameters are compared with previously reported CuO-based glucose sensors and listed in table 2.1. It can be seen from the table that our results are superior in terms of a combination of sensitivity, linear range, and detection limit. We have observed that the linear ranges for glucose level depend on NaOH concentration (pH level) [41], [39], [64], [110], [118].

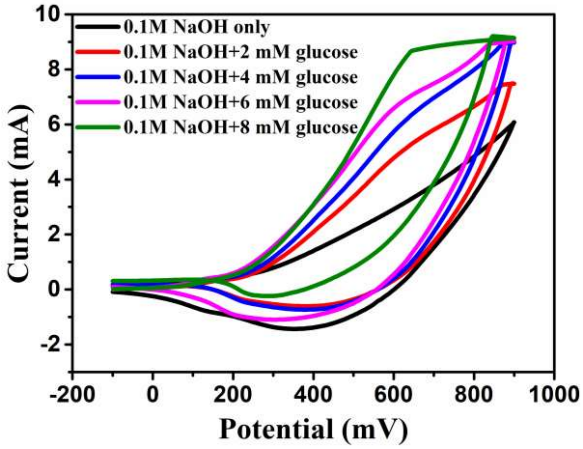

Figure.2.15. C-V plots of Au modified CuO NWs electrode at a different concentration of glucose from 0 mM to 8mM.

It is seen that the lower linear range was found in the case of 0.1 M NaOH solution[3], [20], [26], [32]where as a higher linear range in the case of (0.5M and 1M) NaOH solution. The results obtained are 'promising compared with other reports in terms of linear range, the sensitivity of 4398.8 µAmM-1cm-2 and detection limit of 0.5 µM [3], [20], [26].

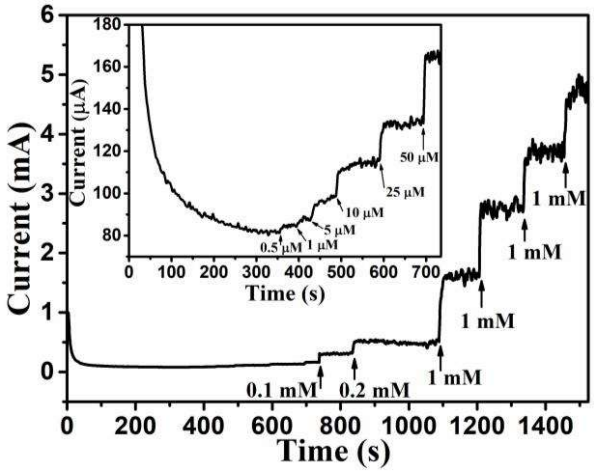

Figure.2.16. Transient current responses of Au NPs modified CuO NWs at 0.6 V with successive addition of glucose (0.1 mM, 0.2 mM, 1 mM, 1 mM,1 mM, and 1 mM). Transient response with a low concentration of glucose (0.5 µM, 1µM, 5µM, 10µM, 25µM, and 50µM) is shown in the inset of the figure.

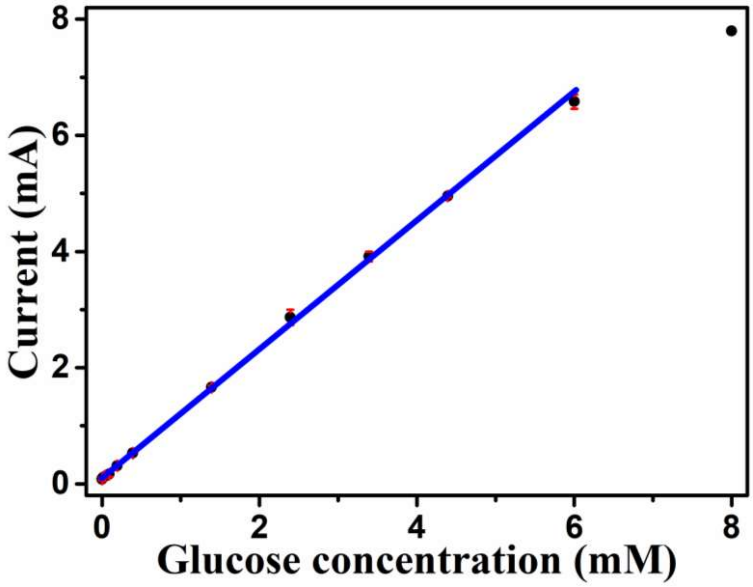

Figure.2.17. Sensitivity plot of Au modified CuO NWs electrode for the different concentration of glucose from 0.5 µM to 8 mM.

2.3.7. Glucose Sensing at higher Concentration of NaOH

It cannot be ignored that most of the earlier reports (independent of the chemical nature of the catalyst) showed the maximum of the linear range of <10 mM glucose at lower alkali concentration of the electrolytes. This sub 10mM glucose detection may be sufficient for a healthy to marginally higher glucose level but not for diabetic patients or higher glucose levels. Moreover, beyond this linear range of amperometric detection, a nonlinear increase in the current followed by saturation is also observed in most previous studies, which are useless for accurate measurements. Hence the extension of this linear range is non-trivial. A recent publication [119] shows that it can be incidentally attained by higher OH- concentration due to mechanistic changes in the underlying detection chemistry. It has been shown, albeit, with CuO catalyst that

glucose transforms to en-diol format higher OH- concentration, which reduces the barrier of electro-oxidation reaction, and a 4-electron transfer reaction is initiated to generate higher current hence higher activity. The final product is gluconolactone. This is contrary to the traditional response involving 2e- transfer process to develop the final product as gluconolactone.

Working Electrode:

$$CuO + H_2O + 2OH^- \rightarrow Cu(OH)_4^- + e \quad (2.3)$$

High pH : $C_6H_{12}O_6$ (Enediol) $+5OH^- \rightarrow C_6H_9O_7$(glucuronate) $+ 4e + 4H_2O$ (2.8)

Low pH: $C_6H_{12}O_6$ (glucose) $+3OH^- \rightarrow C_6H_{11}O_7$(gluconolactone) $+ 2e + 2H_2O$ (2.9)

Counter Electrode:

$$2H_2O + 2e \rightarrow H_2 + 2OH^- \quad (2.10)$$

To the selection better electrode, the different copper oxide was chosen like Cu $(OH)_2$ NWs, CuO NWs, and CuO NWs with GNP. The current which is observed in the case of Cu(OH)2 NWs was very low, moderate for CuO NWs, and extremely high for CuO NWs with GNP in the solution of 0.5M NaOH and 1mM glucose concentrations. Due to the very high current observed in CuO NWs with GNP, we used it as a working electrode for current research work. The drastic improvement with CuO NWs with GNP is due to intensive increments in surface-to-volume ratio for CuO NWs with GNP electrodes. The Cyclic voltammeter (CV) graph of the different working electrodes is shown in Figure. 18(a). CuO NWs with GNP electrodes are dipped in the solution of 0.5M NaOH with varying glucose concentrations at 0mM, 1mM, 2mM, 3mM, 4mM, and 5mM. It is observed that the current increases with an increase in glucose concentration, and linearity are found to be maintained, as elucidated in Figure.2.18 (b).

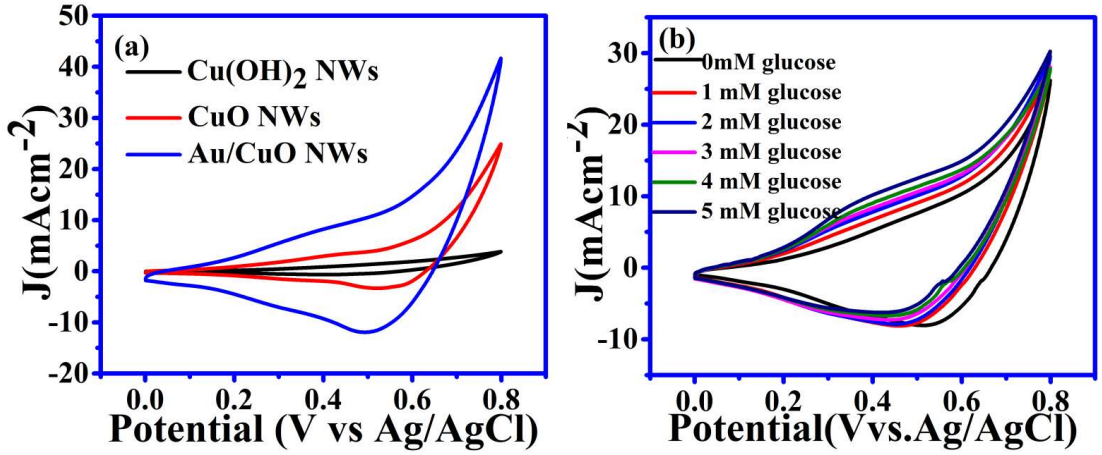

Figure2.18.C-V curve of the electrode.(a) Current density versus potential graph for different type of electrode (b)Current density of CuO NWs electrode with different concentration of glucose from 0 to 5mM

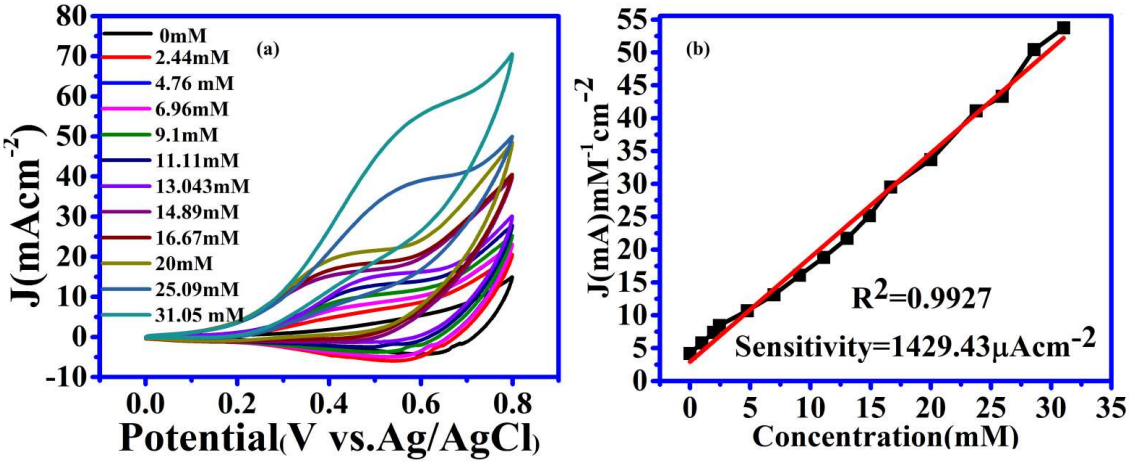

Figure2.19: (a) C-V graph at 0.5M NaOH solution with successive addition of glucose from 0 mM to 31..05 mM glucose solution (b) Linearity graph between current density and concentration at 0.55 V of the reference voltage

Figure.2.19 (a) again shows the CV plot same as figure 2.18(b), which covers the complete glucose range for the working electrode at a solution concentration of 0.5 M NaOH up to 31.05mM, which linearity is maintained. The final relation between current and concentration is shown in Figure.2.19 (b). It shows the sensitivity of the sensors 1429.43 $\mu Acm^{-2}mM^{-1}$ with R^2=0.9927 and linearity shows a maximum value of 31.05 mM.

The current-voltage graphs for the GNPs modified CuO NWs based electrodes with different scan rates are shown in Figure.2.20 (a). This figure confirms the redox reaction model. The linearity graph of the cathodic peak current and anodic peak current with different scan rates ($5mVs^{-1}$ to 500 mVs^{-1}) is shown in the figure. 2.20(b). Because of the above discussion, it can be easily observed that the redox reaction model is the surface-confined process [120]-[121], and the glucose molecule directly oxidizes the composite surface of CuO NWs with GNP. The electrons were directly transferred without any mediators. The studied electronics properties over the surface are an essential tool for the measurements of the electrochemical impedance spectra (EIS).EIS measurements clearly are shown in Figure.2. 21(a) depicts the gradual enhancement of conductivity from Cu (OH) 2 NWs followed CuO NWs-GNP electrode. Figure.2. 21(a) also reveals that the resistance is reduced, and conductivity is enhanced due to the decoration of gold nanoparticles on CuO NWs. EIS measurements were performed by considering a frequency range from 105 Hz -0.1Hz with an open circuit potential of 26mV. Nyquist plot of the (Cu (OH)2) NWs, (Au/Cu (OH) 2) NWs, Copper Oxide (CuO) NWs, and CuO NWs with GNP are shown in Fig. 2.21(a). The smallest semicircle of CuO NWs with GNP clearly shows the lowest resistance and higher conductance which confirms the accelerated rate of electrons transfer in the presence of gold nanoparticles. Uric acid (UA), ascorbic acid (AA), dopamine (DA), sucrose, lactose, and maltose are the various interfering components along with glucose present in human blood serum. The glucose concentration in human blood serum is approximately 30 times more than the above components of the above interference [122]. Due to the reasons described above, the selectivity of CuO NWs with GNP electrode-based glucose sensor under study was examined at 1mM glucose with these

interfering species of 0.2 mM each of lactose, sucrose, and maltose, UA, AA, and DA. Due to increased oxidation of glucose in comparison to other interferences components, the change in current was significantly great for glucose in comparison to other interfering species, which is as shown in figure 2.21(b).

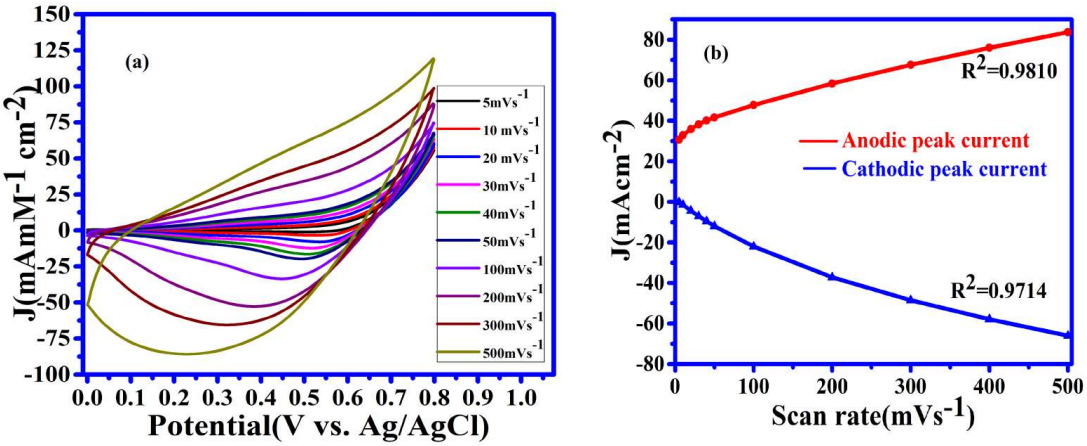

Figure2.20:(a) Electrochemical characterization (a)C-V obtain at 1mM glucose in 0.5M NaOH solution at different scan rates.(b) the graph between peak current density versus scan rate .

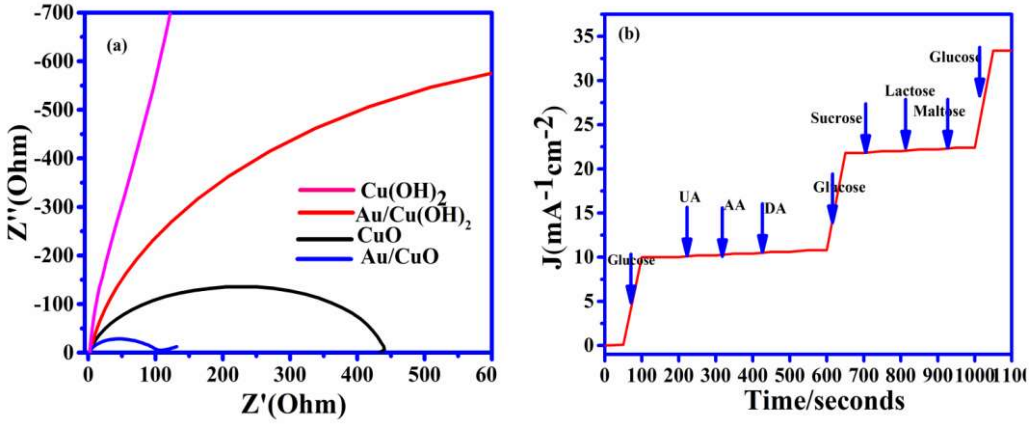

Figure2.21(a).Nyquist plot for different copper electrode $Cu(OH)_2$NWs,Au/CuO NWs, CuONWs,and Au/CuO NWs at OCP(open circuit potential) (b) Anti-interference property of the CuO NWs decorated by GNP electrode with 1mM of glucose and with 0.1 mM each of UA,AA,and DA.then 1mM of glucose with 0.05mM sucrose, lactose, and maltoseand 1mM of glucose added in the last.

At the concentration of 1M NaOH solution, working electrodes CuO NWs with GNP were used for measuring the current with an increase in glucose concentration. At a fixed voltage of 0.55 volt, the increment in current was directly proportional to the amount of glucose added to the solution.

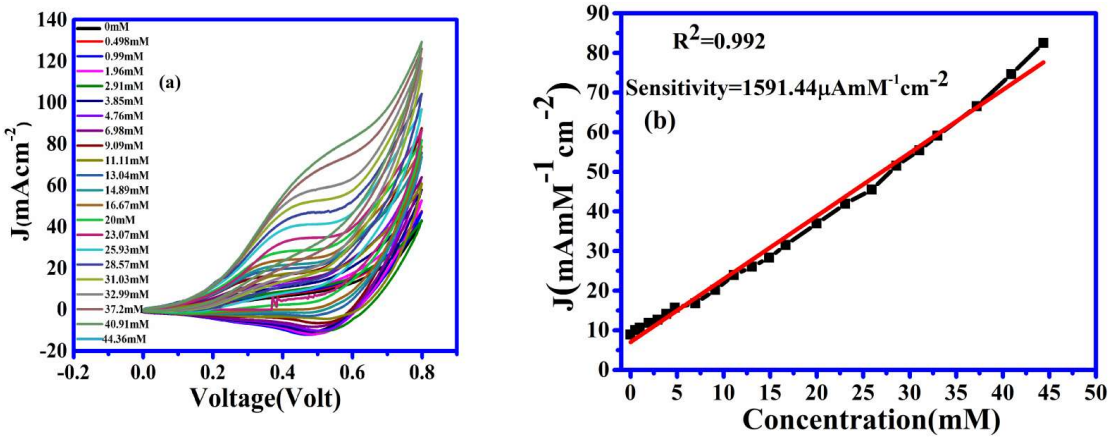

Figure2.22: (a) C-V graph at 1M NaOH solution with successive addition of glucose from 0 mM to 44.36 mM glucose solution (b) Linearity graph between current density and concentration at 0.55 V of the reference voltage

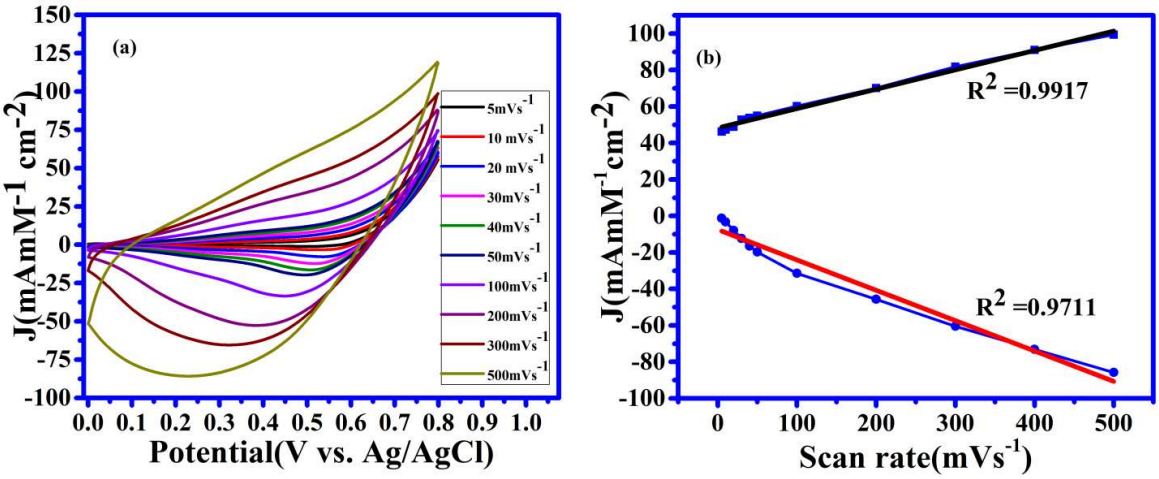

Figure2.23 (a) C-V graph with 1M NaOH solution and 1mM glucose concentration with different scan rates.(b) The linearity graph between current density and potential with different scan rates

The sensitivity and linearity of the different Au-nanoparticles decorated CuO NWs (working electrode) has been given in Table2.2. From Table2.2, it can easily conclude

that at 0.5M and 1M NaOH concentration, this sensor works for the severe diabetic patient (linearity up to 31.05mM and up to 44.36mM) with good sensitivity.

Table 2.2: Comparasion of the Non- Enzymatic Glucose Sensors baasd on Direct Modification of Working Electrode at Different Concentration of NaOH.

Sample	**Sensitivity ($\mu AmM^{-1}cm^{-2}$)**	**Linear Range(mM)**	**Detection Limit(µM)**	**Solution Concentrations(M)**
CuO NWs with(GNP)[123]	4398.8	0.005-5.9	0.5	0.1
CuO nanowires/ copper foam[41]	2217.4l	0.001-18.8	0.3	1
Au/CuO nanocauliflower [97]	708.7	0.001-30	0.3	1
3D Cu@ Cu_2O aerogels[76]	194.88	0.001-17.12	0.6	0.1
Cuo Nano Particles/Ink jet[124]	2762.5	0.05-18.45	0.5	0.0001
ZnO Nano rod decorated by CuONPs [116]	2961.8	0.001-8.45	0.40	0.1
CuO NWs with Au NPs**(This work)**	1425.69	0.001-31.05	0.3	0.5
CuO NWs with Au NPs **(This work)**	1591.44	0.001-44.36	0.3	1

2.3.8. Reusability, Reproducibility, and Stability Tests

The critical factors for measuring the efficiency of the sensing devices are reusability, reproducibility, and stability. For the reusability, CuO NWs with the GNP electrode was dipped into a freshly prepared sample containing one mM of glucose in 0.5M NaOH solutions at 50 mVs−1 scan rate, and the resultant data were shown in Figure 24(a) and 24(b).

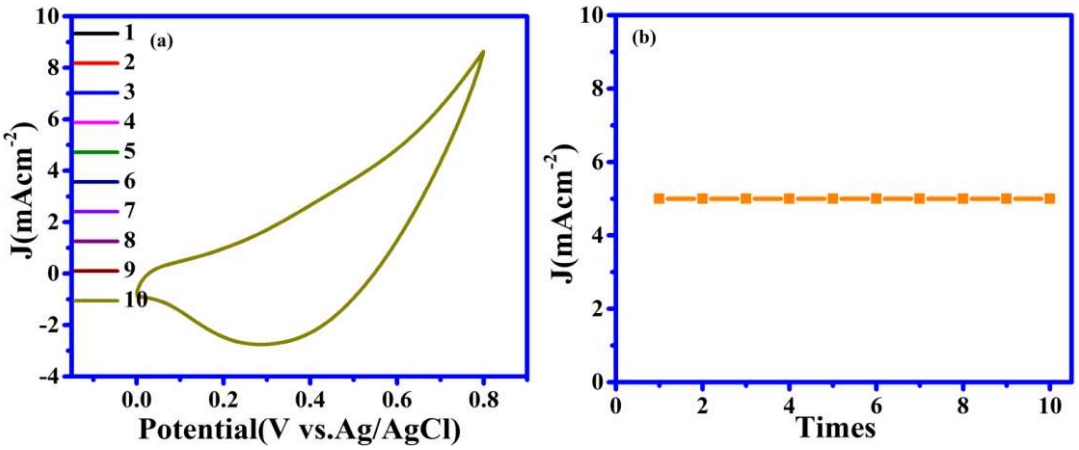

Figures 2.24:(a) Reusability graph between at 0.5M NaOH and 1mM glucose concentration (b) constant current of 5mA obtained at 0.55vollt potential

The electrode was dipped in the solution at least ten times in the same solution or ten different solutions. It was observed that CuO NWs GNP glucose sensing electrode retains more than 99% of its original response, which shows its reusability. To test reproducibility, ten freshly prepared Au/CuONWs with GNP electrode was used in 1mM of glucose solution of 0.5M NaOH with a scan rate of 50 mVs^{-1}.Each electrode's peak current is mentioned in the C-V graph, as shown in Fig. 2.25(a) and (b). The response of these electrodes is found to have a relative standard deviation of 5%. It can be concluded from the above discussion that the sensors based on CuO NWs with GNP electrodes are good enough to reproduce approximately the same results hence shows the sensor's reproducibility. To add more functionality to the sensors, the stability test was evaluated by the CV response of the CuO NWs with the GNP electrode at an interval of 3 days for a month, as shown in Fig.2.26 (a). The electrode was stored at room temperature up to the completion of the measurement. After the completion of 30

days, the response of the proposed CuO NWs with the GNP electrode was compared with the response of the electrode on the first day.

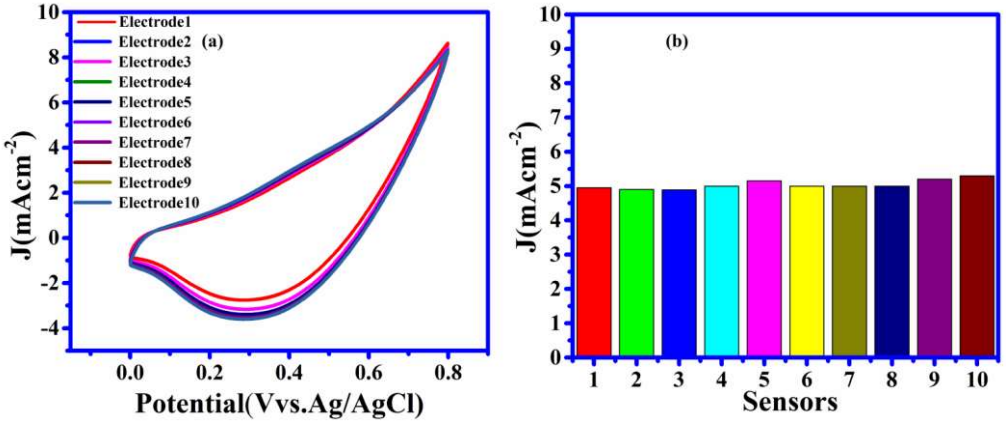

Figure2.25.(a) Reproducibility graph from 1 electrode to 10 electrode after 1mM addition of glucose(b) The histogram curve at 0.55V potential and 1mM glucose

The result is shown in Fig 2.26(b) as a histogram plot which conveys the information that the proposed sensor is much stable which can retain 95 % (measured on day 30) of its originals response (measured on day 0). The excellent stability response of the electrode was due to the stable grown of CuO NWs with GNP on the surface of the electrode, which provides strong mechanical stability to the sensing device.

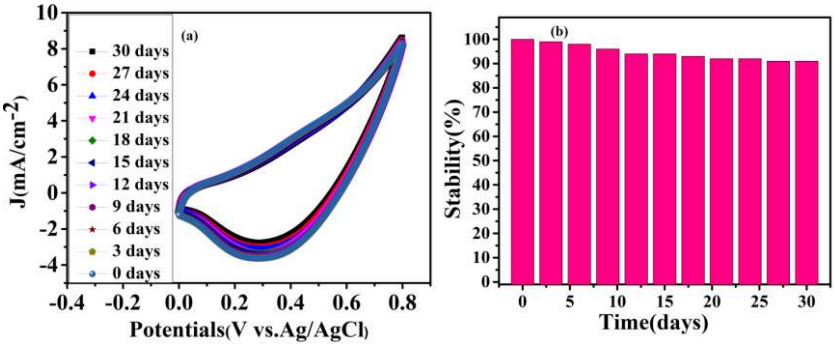

Figure2.26.(a) C-V graph between taken between the interval of 3days and up to 30 days (b) corresponding histogram from 0 day up to 30 days with interval of 3 days.

2.3.9. Measurement of Glucose in Human Serum Samples

It is also investigated with human blood serum to ensure the viability of this reported glucose sensor is in practical relevance. The human blood serum contains glucose, and it can be determined in the measurement. The blood samples have been collected with the help of the university students' health center (Sir Sundar Lal Hospital, Banaras Hindu University, and Varanasi, India) with tested blood sugar levels. The blood samples are of the healthy person had been taken from our research group. About 100 µL of blood was added into 9.90 ml of 0.1 M NaOH. The corresponding oxidation current response is measured at 0.6 V. The sugar concentration in a blood sample is evaluated using the reference current through a calibration curve obtained from the electrochemical measurement. The received transient response of the sensor for human blood serum, and linearity plot is shown in the figure.2 27.

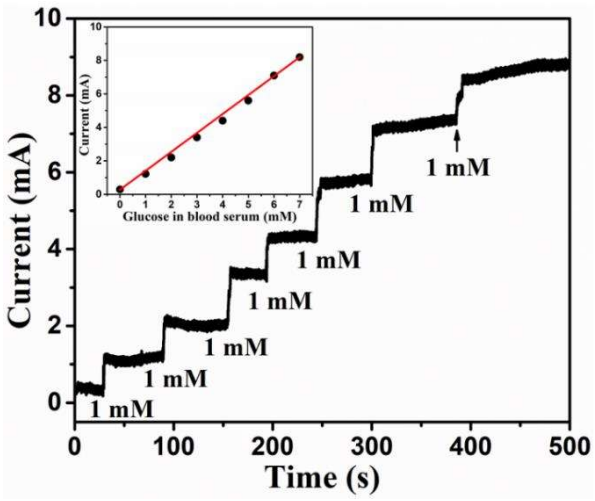

Figure.2.27. Transient response of Au NPs modified CuO NWs electrode at 0.6 V with successive addition of human blood serum corresponding to 1 mM glucose. The nearly linear glucose response of blood serum in the inset.

The slight blurred and the higher current response is obtained in the case of human blood serum. This is because the presence of various interference apart from glucose in the blood serum. The glucose response is nearly linear (correlation coefficient less than 0.99), which can measure the glucose level of 130 mg/dl (>7 mM) efficiently. We have compared these results with the expected results provided by the Health Centre. Each sample is measured three times, and the observations are listed in table 3. We can easily match the results with expected results. This determination of glucose concentration can be extended further in the diluted serum samples also. Since the concentration of glucose is reduced when the serum is diluted, the amount of glucose in the diluted serum samples determined by using the proposed method must be multiplied by the inverse factor of serum dilution to obtain the desired result. Thus, the proposed sensor is very effective for glucose detection and could be used in practical relevance. X=Relative standard deviation (RSD) of 3 measurements.

Table.2. 3. Detection of Glucose in Human Serum Sample.

Sample	Glucose concentration (mM) Spectrophotometric method (provided by the health center)	Proposed method	Recovery (%)	RSD [X] (%)
1	6.178	6.13	99.22	0.5
2	5.238	5.35	97.90	1.5
3	4.741	4.91	96.56	5.2

2.4.Conclusion

A non-enzymatic glucose sensor with easy fabrication steps is summarized in this chapter. The gold nanoparticles (Au NPs) were deposited on CuO NWs electrode using an in-situ chemical reaction. These Au NPs on the surface of CuO NWs increase the electrode's effective surface-to-volume ratio, increasing the catalytic property of the Au NPs modified CuO NWs significantly compared to that of the bare CuO NWs. As a consequence, the oxidation and reduction properties of the Au NPs changed CuO NWs are increased drastically. The enhanced aforementioned properties of the Au NPs modified CuO NWs electrode have been explored for improving the detection capability of the CuO-based glucose sensors. The Au NPs modified CuO NWs based glucose sensor understudy in 0.1 M NaOH solution gives a sensitivity of 4398.8 μAmM-1cm-2 with maximum linearity up to 5.9 mM, which is promising among the reported results for the CuO based glucose sensors. This electrode was used for a higher concentration of solvent (0.5M and 1MNaOH). This extended concentration of NaOH solvent (0.5M NaOH and 1M NaOH) results gives a sensitivity of 1440.63 μAmM-1cm-2 and 1591.44 μAmM-1cm-2, respectively. The linearity ranges of the glucose sensor are 31.05 mM and 44.36mM at 0.5M and 1M NaOH solvent concentrations. The low detection limit of the sensor at different concentrations shows that the sensors can be used to detect extremely low glucose levels in saliva and urine. The results reported here are accurate and stable up to our understanding. The proposed glucose sensor was also used for measuring the amount of glucose in human blood in a realistic situation.